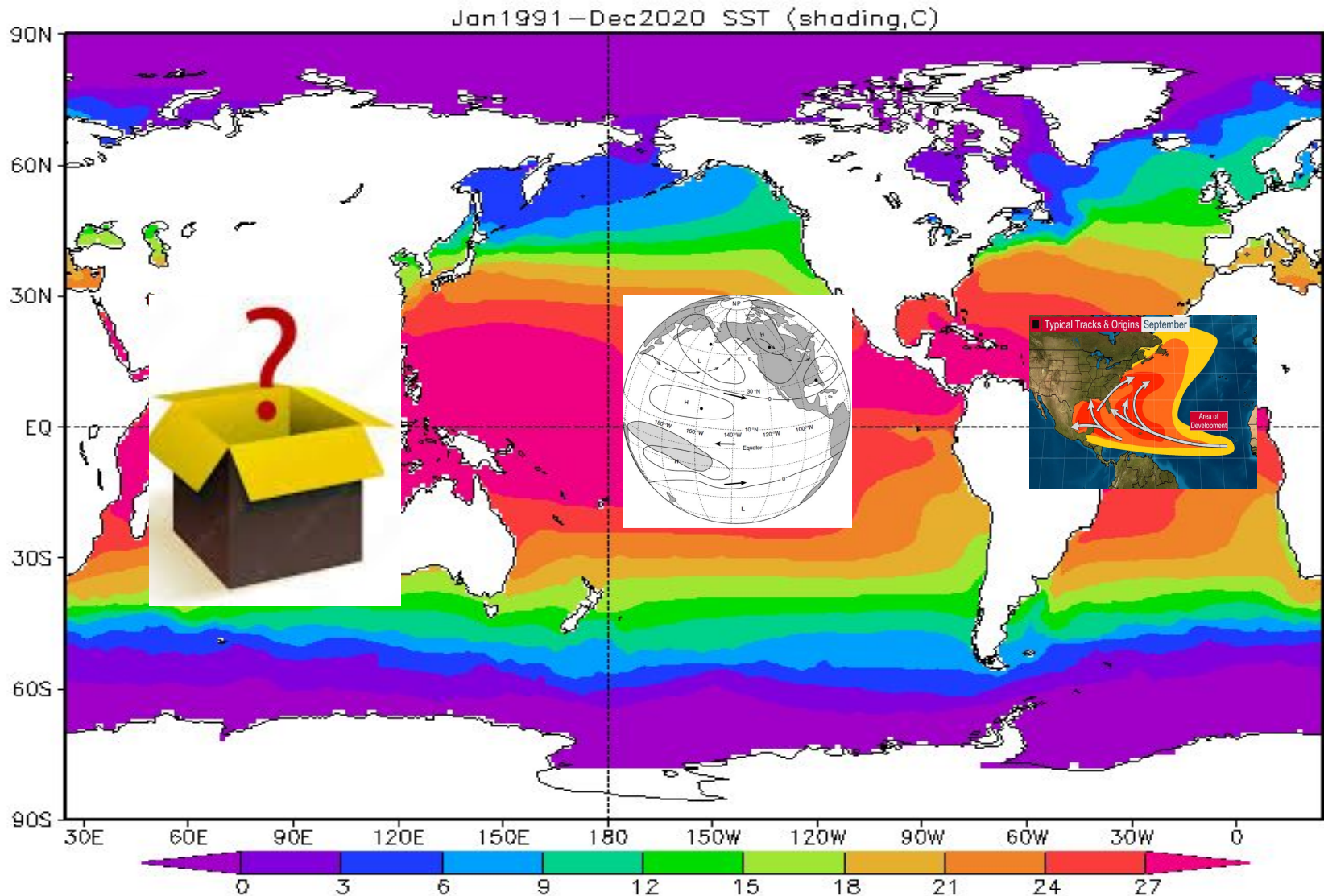


- (a) ENSO affects U. S. through generating a PNA-like teleconnection;
- (b) The tropical N. Atlantic Ocean influences hurricane and eastern U. S. climate;
- (c) Is there any impact of the Indian Ocean on U. S. climate?**



# The Impact of the Tropical Indian Ocean on U. S. Winter Precipitation

Zeng-Zhen Hu

Arun Kumar, Bhaskar Jha\*, Mingyue Chen, and Wanqiu Wang

NOAA/NWS/NCEP/Climate Prediction Center

College Park, MD 20740, USA

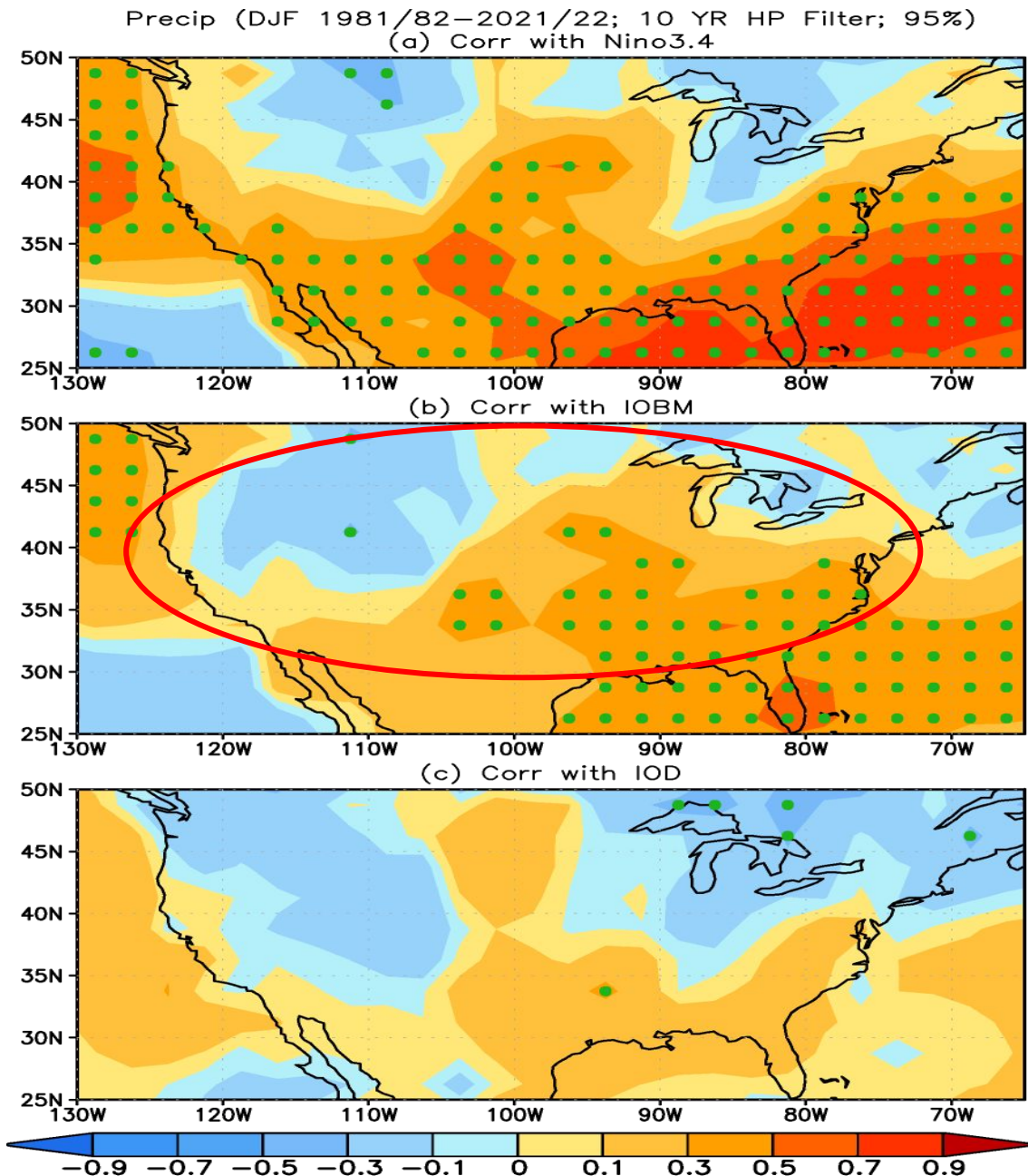
\*ERT, Inc

NOAA's 48th Climate Diagnostics & Prediction Workshop  
Tallahassee, Florida, USA; 26–29 March 2024



# Objectives:

- Are there any influences of the Indian Ocean (IO) on U. S. climate?
- What is the physics leading to the influence?
- What are the differences of the impacts of ENSO and IO on U. S. climate?
  
- *Through observational diagnoses and model forecasts as well as AMIP simulation, we identify the possible influence of IO on U. S. winter precipitation & examined mechanism.*



□ ENSO: a north-south opposite variation pattern.

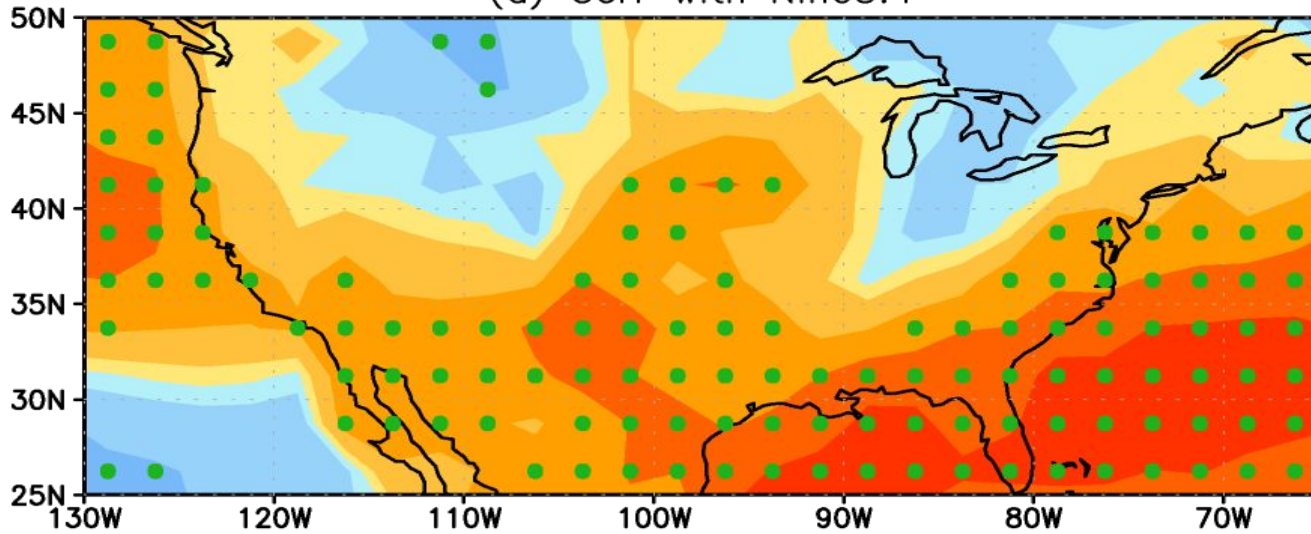
□ IOBM: a northwest-southeast contrast pattern.

□ IOD: weaker and mostly insignificant.

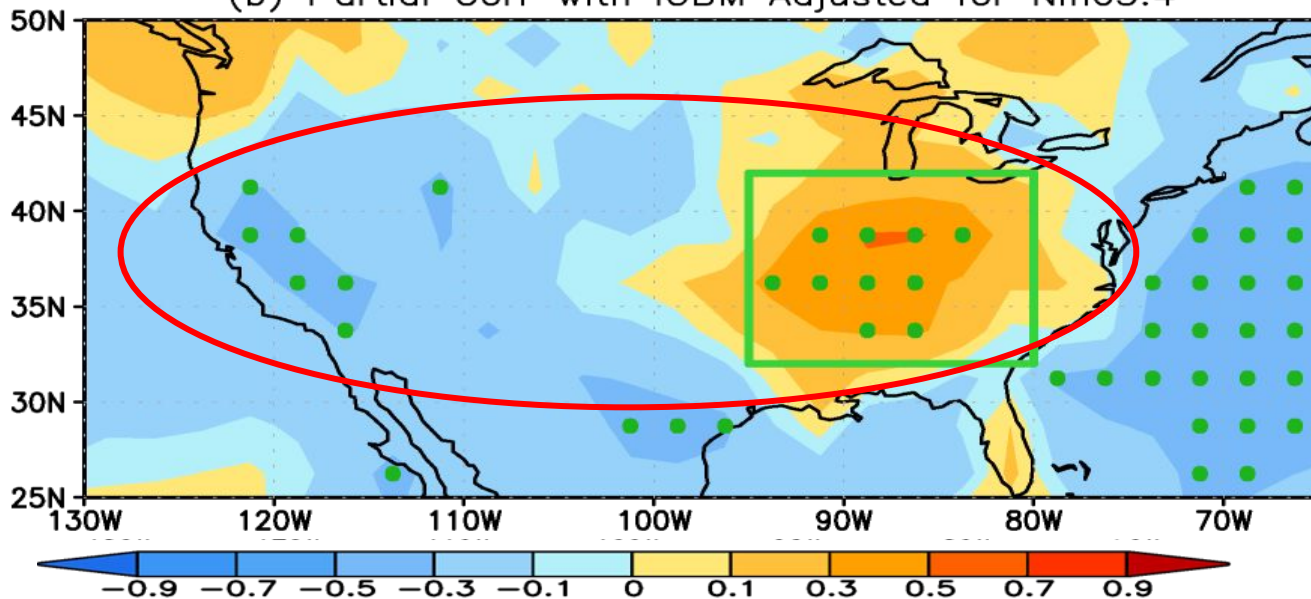
Fig. X: Simultaneous correlations of DJF precipitation anomaly with (a) Niño3.4, (b) IOBM, and (c) IOD indices in DJF 1979/80-2021/22. The data are 10-year high pass filtered. The dots represent significant correlations at the significance level of 5% using the T-test.

Precip (DJF 1981/82–2021/22; 95%)

(a) Corr with Nino3.4



(b) Partial Corr with IOBM Adjusted for Nino3.4

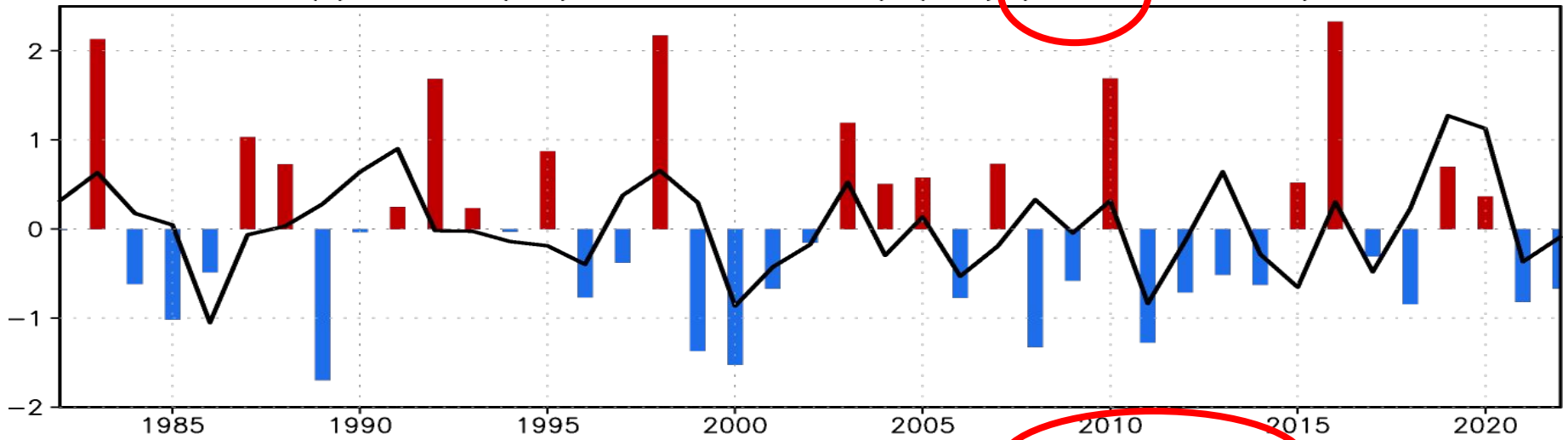


Partial  
correlations  
eliminating  
ENSO  
influence:

□ IOBM: Still a  
northwest-south  
east contrast  
pattern.

Fig. 1: (a) Simultaneous correlations of DJF precipitation anomaly with the Niño3.4 index, and simultaneous partial correlations of DJF precipitation anomaly with the (b) IOBM index adjusted for Niño3.4 index in DJF 1981/82–2021/22. The green rectangle represents the region (32°–42°N, 80°–95°W) to define the southeastern CONUS precipitation index. The dots represent significant correlations at the significance level of 5% using the T-test.

DJF 1981/82–2021/22  
(a) Niño3.4 (Bar) & SE CONUS Precip (Line) ( $r=0.37$ ;  $r^*=-0.06$ )



(b) IOBM (Bar) & SE CONUS Precip (Line) ( $r=0.54$ ;  $r^*=0.43$ )

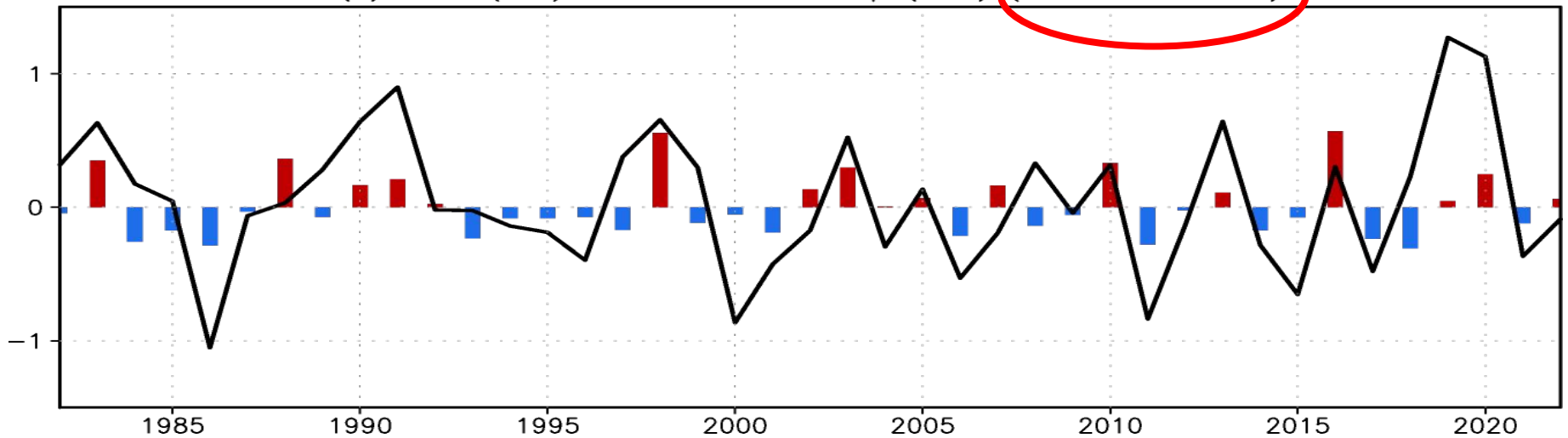
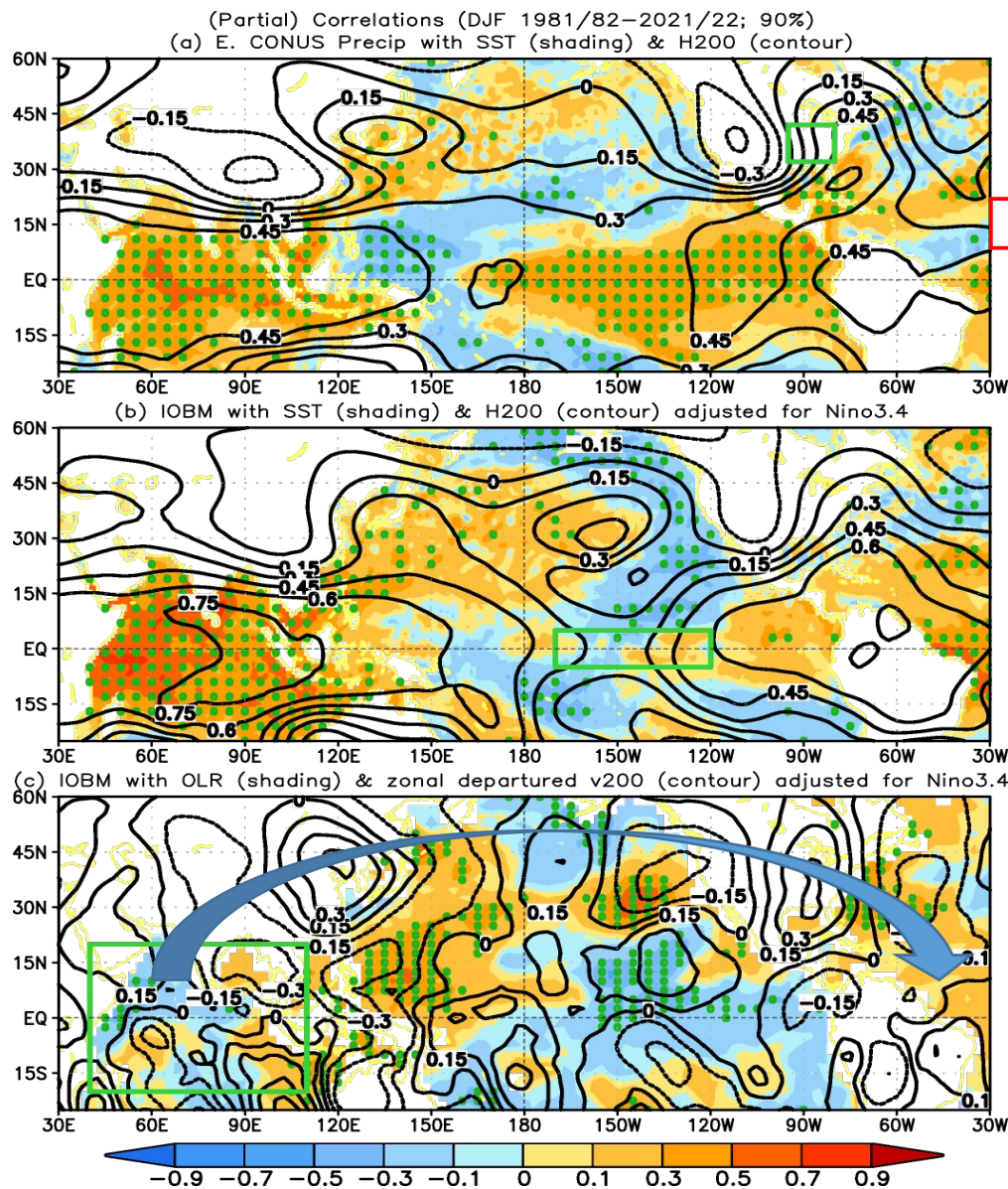


Fig. 2: (a) The southeastern CONUS precipitation index ( $32^{\circ}$ - $42^{\circ}$ N,  $80^{\circ}$ - $95^{\circ}$ W) (curve; unit: mm/day) and the Niño3.4 index (bar; unit:  $^{\circ}$ C); (b) the southeastern CONUS precipitation index (curve) and the IOBM index (bar; unit:  $^{\circ}$ C) in DJF 1981/82-2021/22. The correlation between the Niño3.4 and precipitation indices is 0.37 and the corresponding partial correlation adjusted for the IOBM index is -0.06. The correlation between the IOBM and precipitation indices is 0.54 and the corresponding partial correlation adjusted for the Niño3.4 index is 0.43. The correlations larger than 0.32 (0.41) are significant at the significance level of 5% (1%) using the T-test.

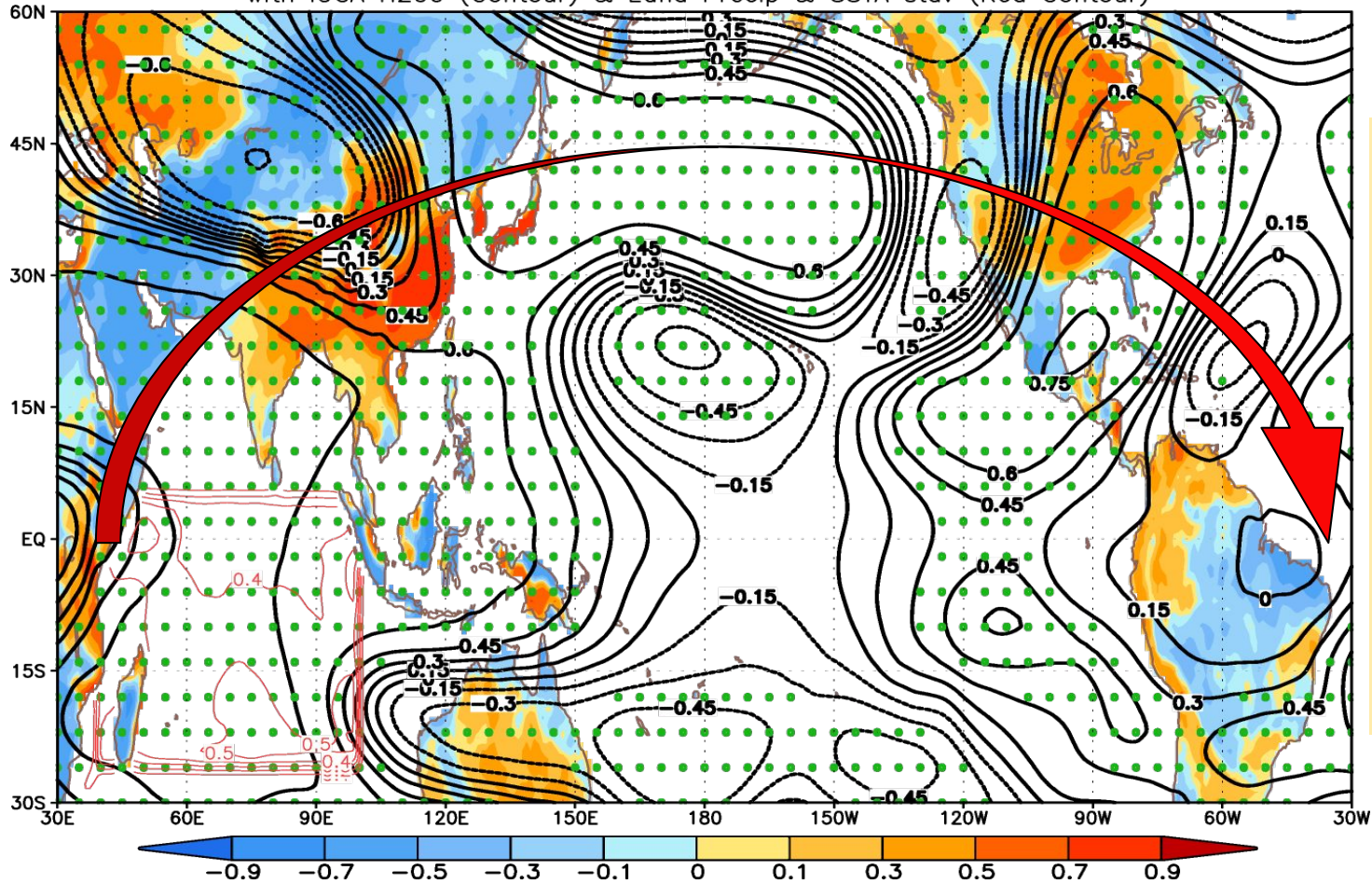
**□ The correlation of SE CONUS winter precipitation with the IOBM index is higher and more significant than that with the Niño3.4 index.**



Physically, the heat conditions in the tropical IO associated with IOBM can generate Rossby wave-like anomalies in the extratropics, affecting SE CONUS winter precipitation.

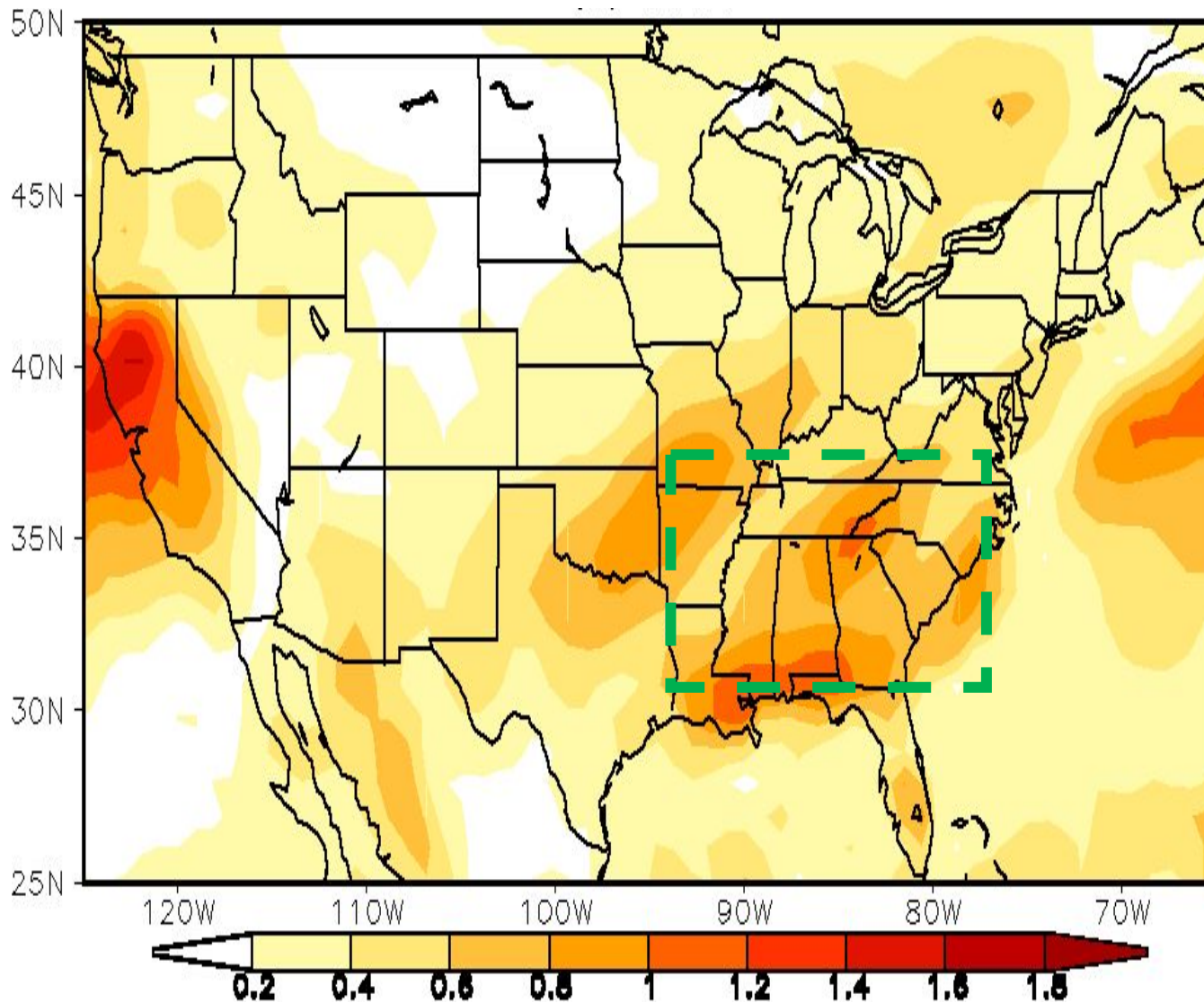
ERA5 data: Fig. 3: (a) Simultaneous correlations of SST (shading) and H200 (contour) anomalies with the southeastern CONUS precipitation index, (b) simultaneous partial correlations of SST (shading) and H200 (contour) anomalies with the IOBM index adjusted for the Niño3.4 index, and (c) simultaneous partial correlations of OLR over ocean (shading) and zonal mean departure meridional wind at 200 hPa (contour) anomalies with the IOBM index adjusted for the Niño3.4 index in DJF 1981/82–2021/22. The dots represent significant correlations (shading) at the level of 90% using the T-test. The contour interval is 0.15. The green rectangles represent the regions to define the indices.

Observed IOBM Index Correlations (DJF 1981/82–2021/22; H200 95%)  
with IOGA H200 (Contour) & Land Precip & SSTA stdv (Red Contour)



IOGA simulations reproduced the connection between IOBM & SE CONUS winter precipitation & the teleconnection.

Fig. 5: Simultaneous correlations of **IOGA simulated** land precipitation (shading) and H200 (black contour) anomalies with observed IOBM index in DJF 1981/82–2021/22. The simulated H200 and precipitation are the ensemble mean of 18 members. The dots represent significant correlations of H200 at the level of 5% using the T-test. The black contour interval is 0.15. The red contour with a contour interval of 0.1°C over the Indian Ocean is the standard deviation of SSTA which represents the SST forcing region used in the IOGA simulations. The multiple red contours across the boundary are associated with sponge-like smoothing of the observed SST specified in the Indian Ocean (25°S–5°N, 38°–100°E) in the IOGA simulations.

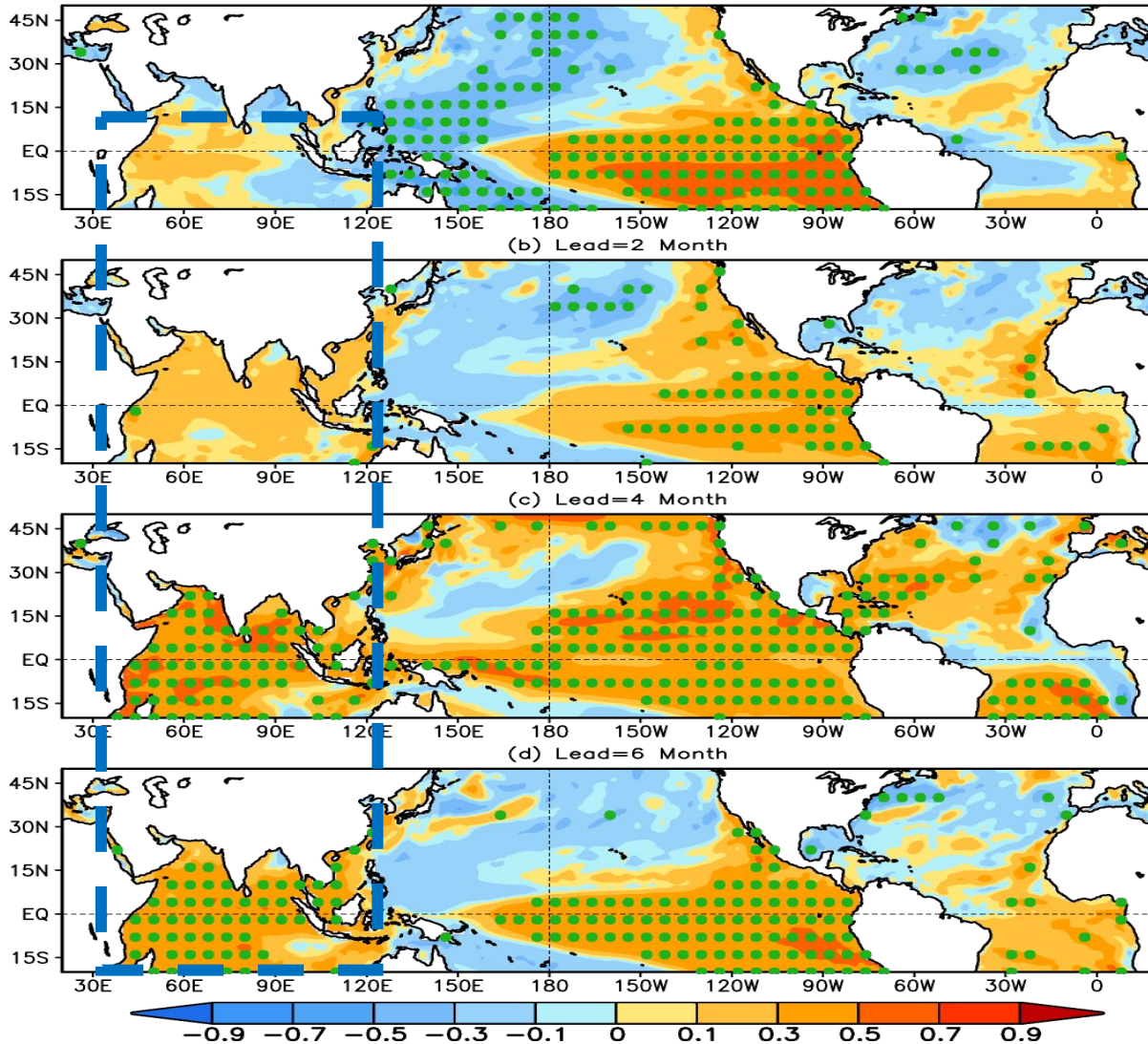


□ Relatively large SNRs are present in SE CONUS in the tropical IO experiment (IOGA).

□ That is generally collocated with significant positive correlations between the winter precipitation and the IOBM index.

*Fig. S3: SNR of precipitation in DJF in the IOGA simulation. The signal is referred to as the standard deviation of the mean of the anomaly of 18 ensemble members, and the noise is the standard deviation of the departure of each ensemble member from the ensemble mean.*

Corr of E. CONUS (32–42N,80–95W) DJF Prec & SST (CFSv2 20 Members; 95%)  
(a) Lead=0 Month

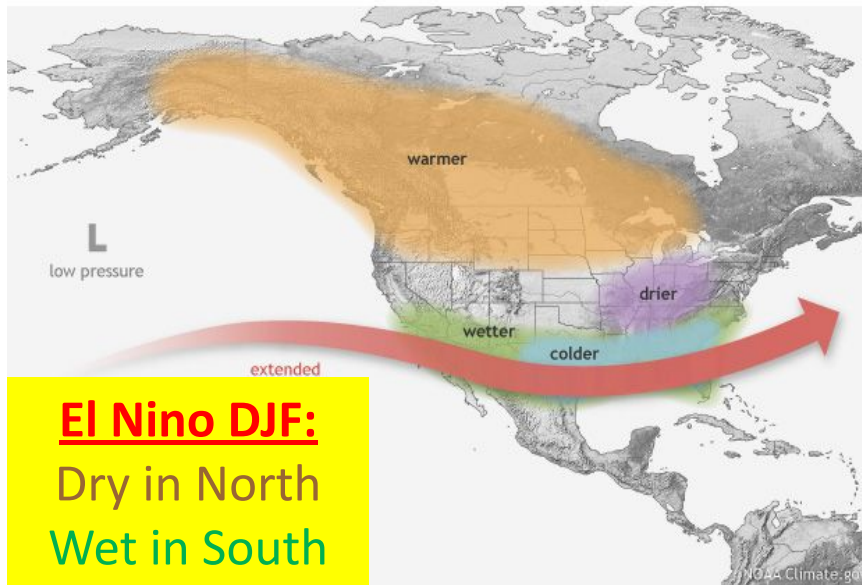


Correlation of SE CONUS DJF precipitation with SSTA in CFSv2 prediction (20-ensemble mean) with different lead time.

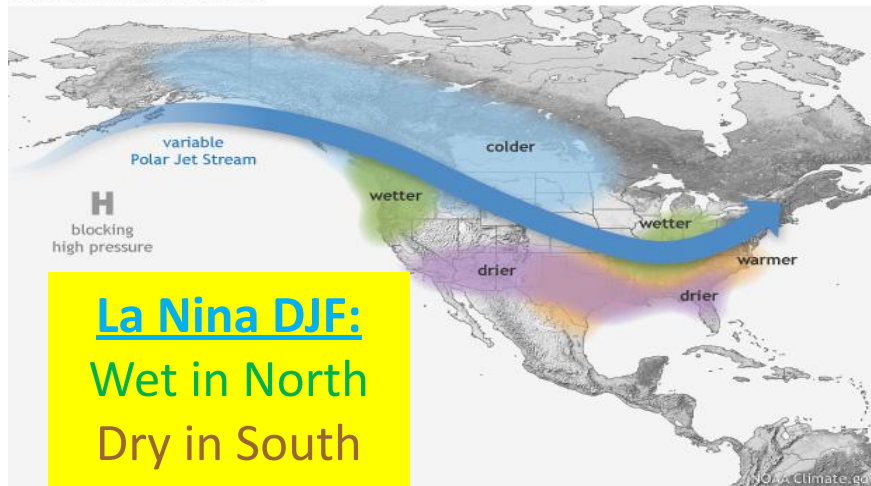
□ CFSv2 **partially** captures the statistical connection between the IO SSTA and CONUS precipitation anomalies in DJF.

Fig. 4: Correlations between the southeastern CONUS precipitation index and SST anomalies in DJF 1982/83-2021/22 of the **CFSv2 forecasts of 20-member** average for lead (a) 0, (b) 2, (c) 4, and (d) 6 months. The dots represent significant correlations at the level of 5% using the T-test.

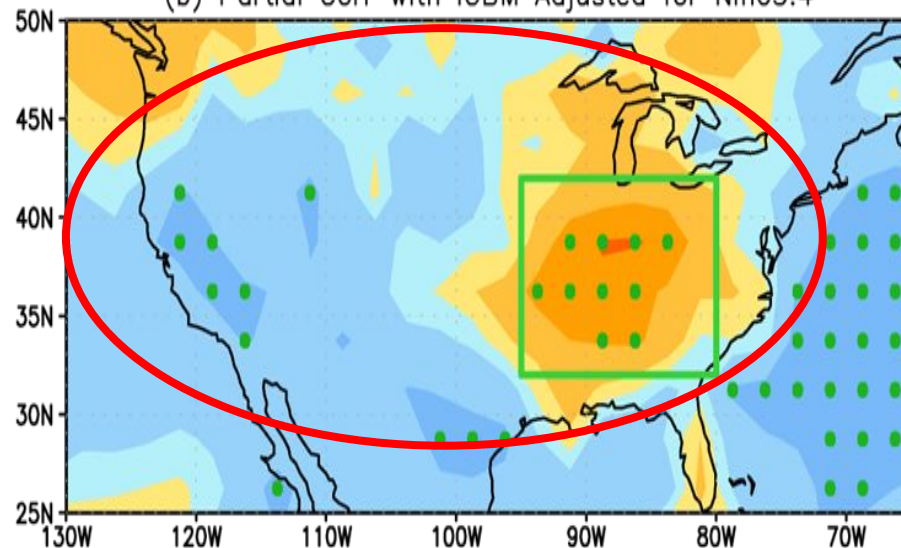
## WINTER EL NIÑO PATTERN



## WINTER LA NIÑA PATTERN



(b) Partial Corr with IOBM Adjusted for Nino3.4



- Different from the north-south opposite sign impact of ENSO on CONUS winter precipitation (left panel), warming (cooling) in the Indian Ocean (IOBM) leads to wet (dry) SE CONUS & dry (wet) NW CONUS.
- The impact of IOBM on SE CONUS winter precipitation is stronger than ENSO.

# Summary and Conclusions

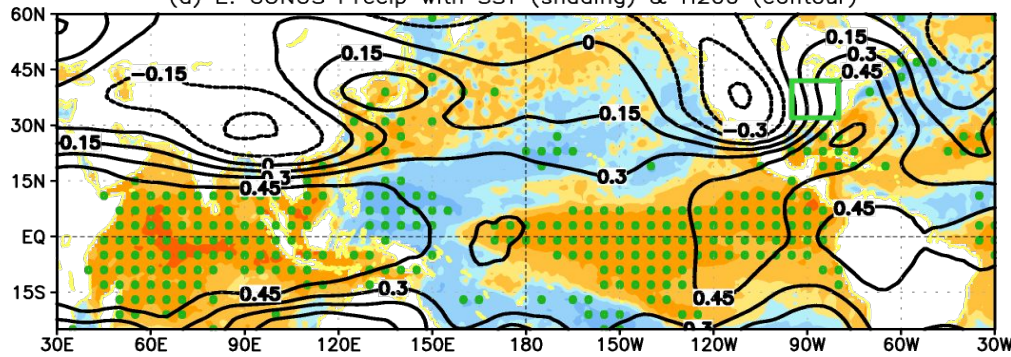
- The impact of the tropical Pacific SSTA associated with ENSO mainly leads to opposite winter precipitation anomalies between S. & N. tiers of CONUS, while the influence of IO basin-wide warming or cooling is mainly in SE CONUS.
- A basin-wide warming (cooling) in the tropical IO is tied to above (below) normal winter precipitation in SE CONUS. IO may play a more important role than ENSO in the *winter precipitation in SE CONUS*.
- IO warming/cooling can excite a wave train expanding from the IO to N. America via Eastern Asia and N. Pacific. Such wave pattern leads to winter climate anomalies in SE CONUS.
- CFSv2 forecasts and AMIP runs reproduce the observed connection between IO and SE CONUS winter precipitation.
- **We may pay more attention to the Indian Ocean in forecast operation and can use the Indian Ocean as a predictor to forecast SE CONUS winter precipitation.**

# Acknowledgements

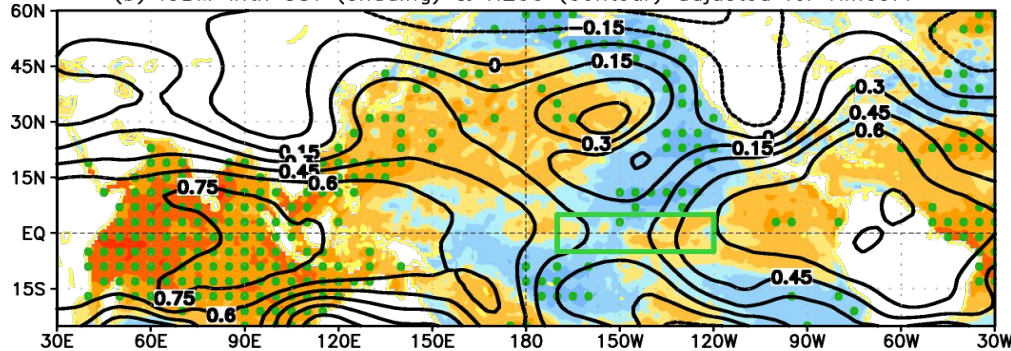
*We appreciate the constructive suggestions from CPC colleagues, Peitao Peng, Hui Wang, Yanjuan Guo, Jieshun Zhu, ...*



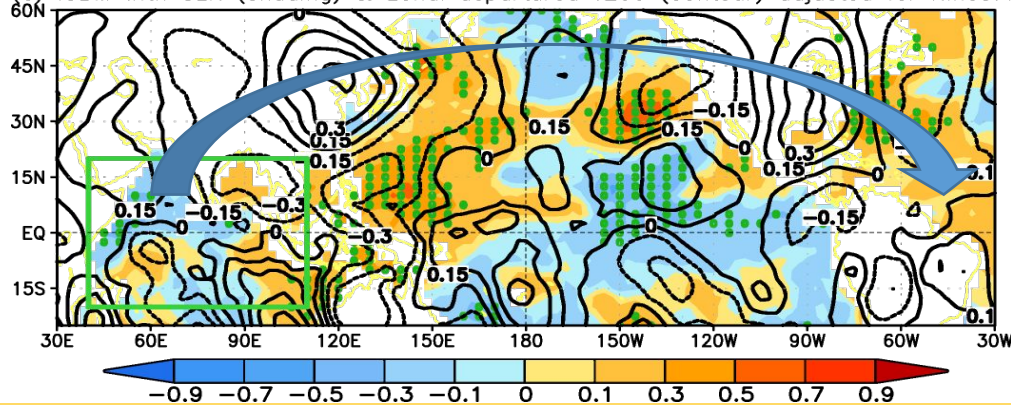
(Partial) Correlations (DJF 1981/82–2021/22; 90%)  
(a) E. CONUS Precip with SST (shading) & H200 (contour)



(b) IOBM with SST (shading) & H200 (contour) adjusted for Niño3.4



(c) IOBM with OLR (shading) & zonal departed v200 (contour) adjusted for Niño3.4

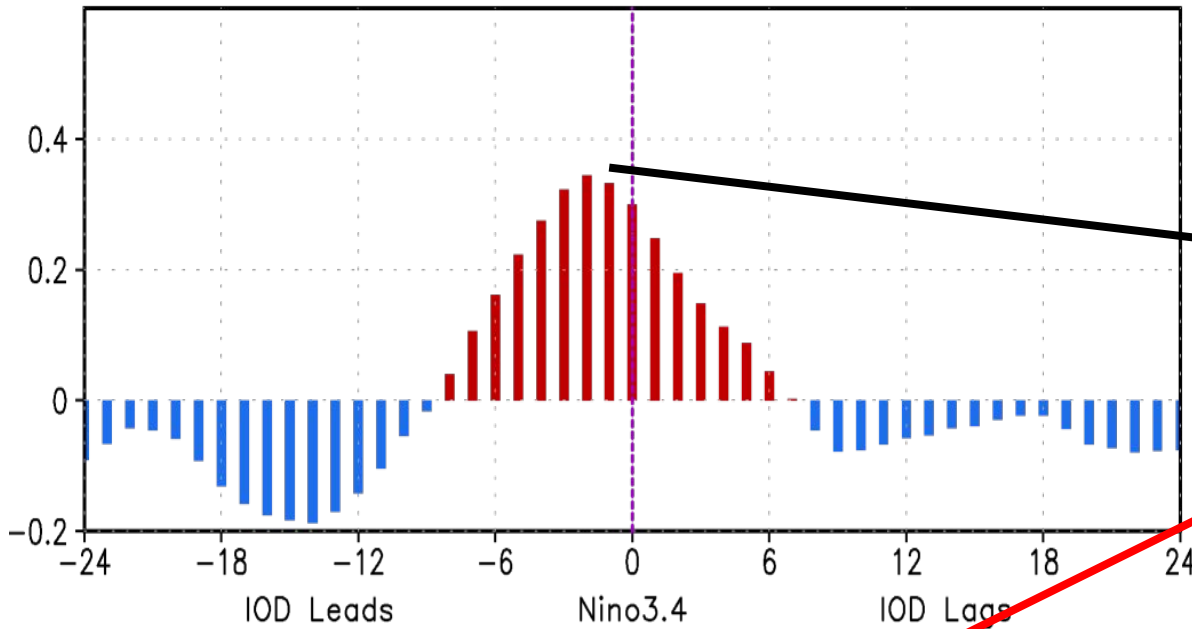


□ Physically, the heat conditions in the tropical IO associated with IOBM can generate Rossby wave-like anomalies in the extratropics, affecting SE CONUS winter precipitation.

ERA5 data: Fig. 3: (a) Simultaneous correlations of SST (shading) and H200 (contour) anomalies with the southeastern CONUS precipitation index, (b) simultaneous partial correlations of SST (shading) and H200 (contour) anomalies with the IOBM index adjusted for the Niño3.4 index, and (c) simultaneous partial correlations of OLR over ocean (shading) and zonal mean departure meridional wind at 200 hPa (contour) anomalies with the IOBM index adjusted for the Niño3.4 index in DJF 1981/82–2021/22. The dots represent significant correlations (shading) at the level of 90% using the T-test. The contour interval is 0.15. The green rectangles represent the regions to define the indices.

Corr (Olv2.1: 1982–2022)

(a) IOD & Nino3.4



□IOD leads ENSO by 1-3 months

□IOBM lags ENSO by 3-5 months

(b) IOBM & Nino3.4

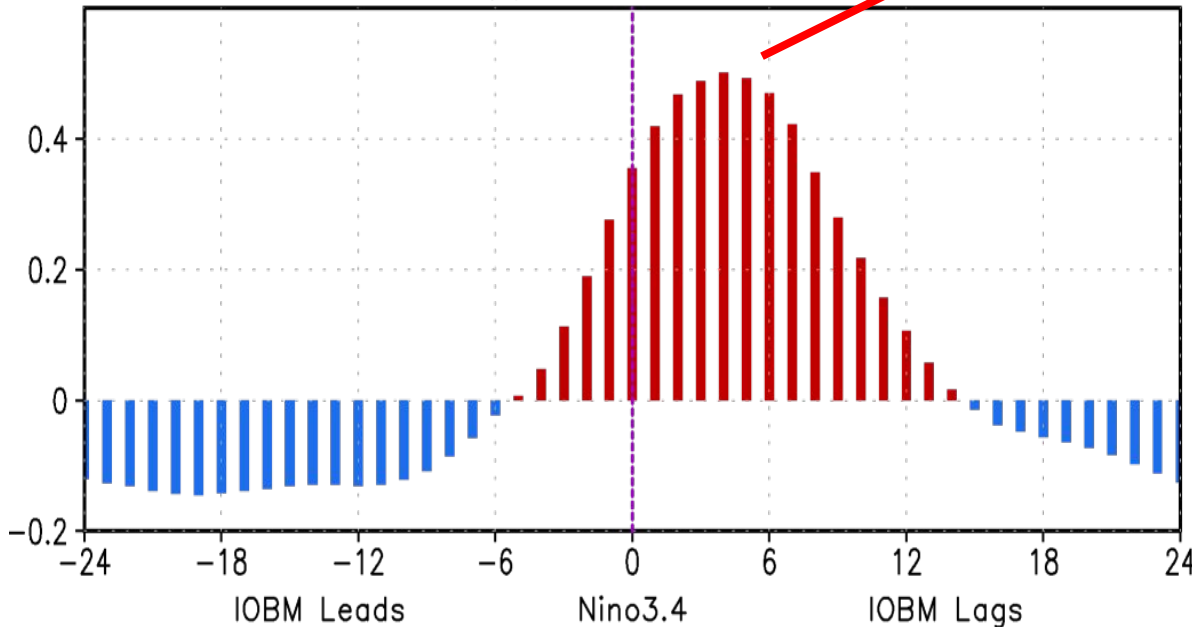
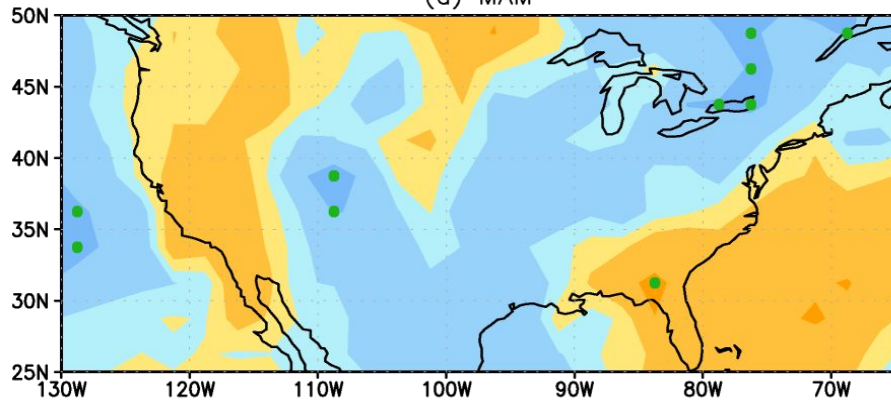


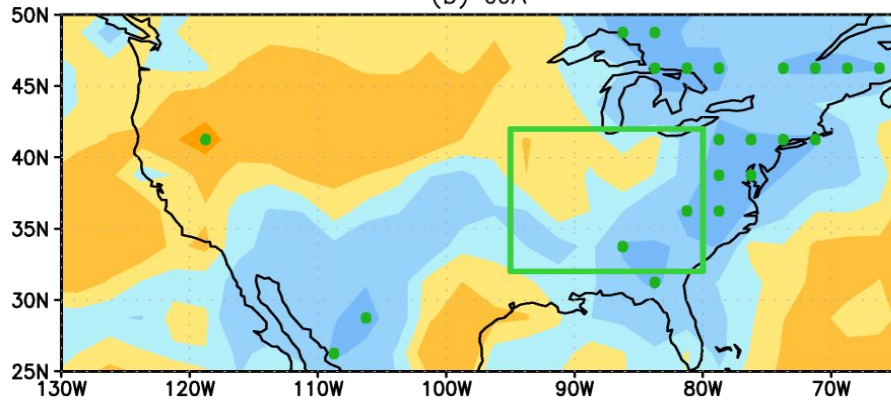
*Fig. S2: Lead and lag correlations between the Niño3.4 index and the (a) IOBM and (b) IOD indices, and (c) between the IOBM and IOD indices in January 1982–December 2022. The negative (positive) numbers in the x-axis denote the number of months of the Niño3.4 index lagging (leading) the IOBM or IOD indices in (a, b), and the number of months of the IOD index lagging (leading) the IOBM index in (c).*

Partial Corr of Precip with IOBM Adjusted for Nino3.4 (1982–2022; 95%)

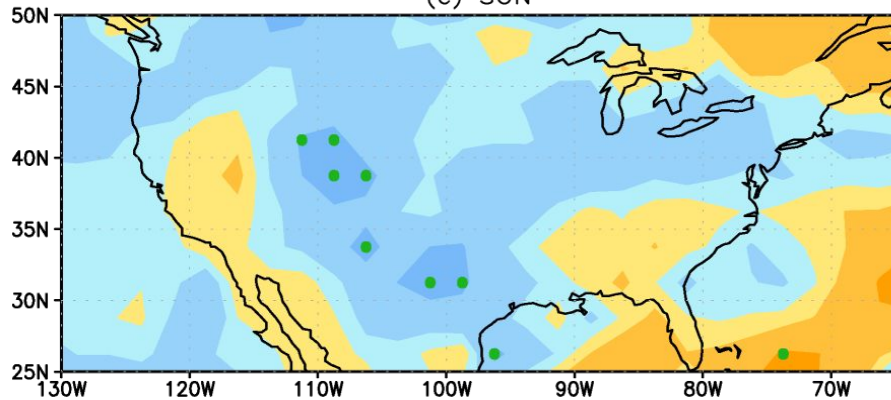
(a) MAM



(b) JJA



(c) SON

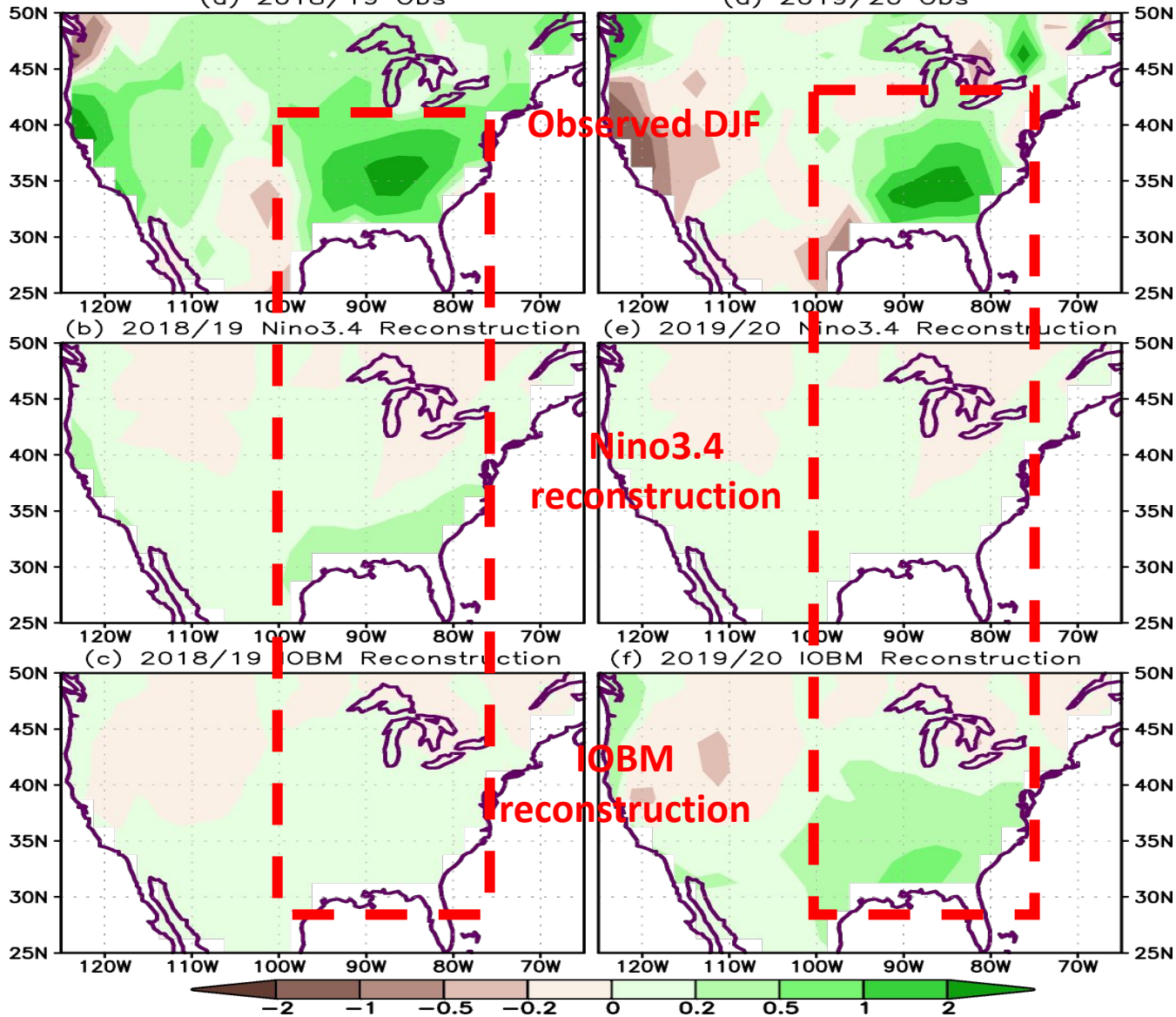


□ No significant (*partial*) correlations between the IOBM and SE CONUS precipitation in the other seasons.

*Fig. S4: Simultaneous partial correlations of precipitation anomaly with the IOBM index adjusted for the Niño3.4 index in (a) March-May, (b) June-August, and (c) September-November 1982-2022. The green rectangle in (b) represents the region (32°-42°N, 80°-95°W) to define the southeastern CONUS precipitation index. The dots represent significant correlations at the significance level of 5% using the T-test.*

DJF Precipitation (mm/day; 10 YR HP)

(a) 2018/19 Obs (d) 2019/20 Obs



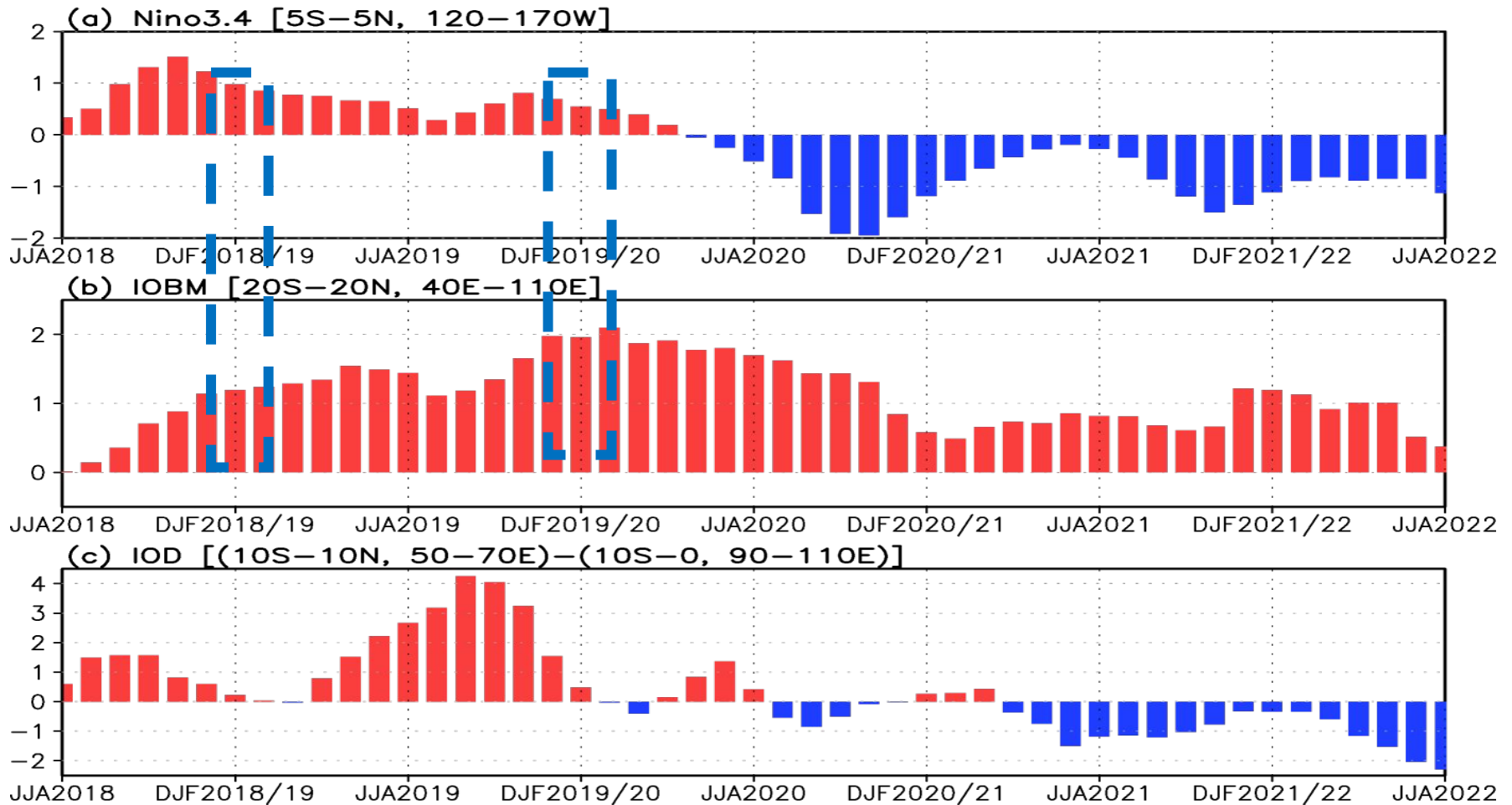
DJF precipitation in 2018/19 & 2019/20:

□ 2018/19 DJF: ENSO played a role.

□ 2019/20 DJF: IOBM had a much larger contribution than ENSO to SE CONUS winter precipitation.

Fig. x: (a) Observed and reconstructed DJF 2018/19 precipitation anomaly (mm) based on the linear regression in DJF 1981/82-2021/22 with the observed (b) Niño3.4, and (c) IOBM indices in DJF 2018/19. Similarly, (d-f) is for the 2019/20 DJF precipitation anomaly. The linear regression is computed with 10-year high pass filtered data.

### 3-Month Mean Normalized SST Indices



- Weak El Niño was present in 2018/19; borderline El Niño in 2019/20.
- In DJF 2018/19, IOBM was smaller positive; Niño3.4 had the larger contribution.
- In DJF 2019/20, IOBM was larger positive and had larger contribution.

Fig. x: Normalized 3-month mean (a) Niño3.4 index, (b) IOBM, and (b) IOD indices from June-August 2018 to June-August 2022.

# IO can affect NAO through a teleconnection pattern

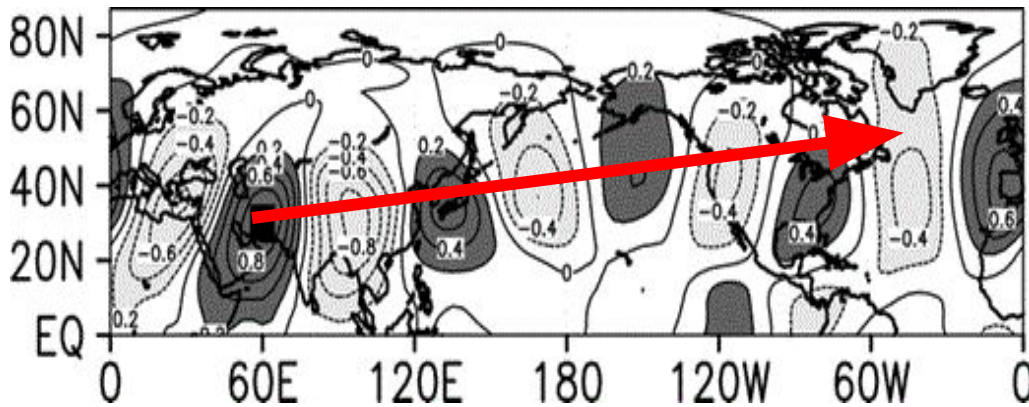


Fig. 5: Correlation of winter (DJF) 300-hPa meridional wind averaged over the black box and winter 300-hPa meridional wind in the Northern Hemisphere.

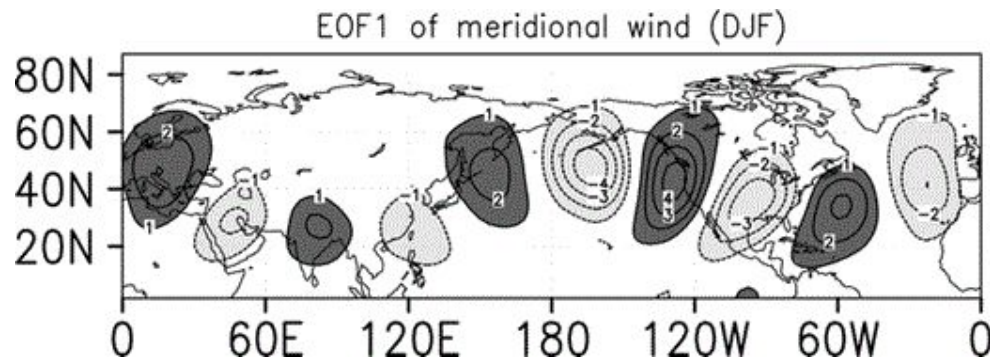


Fig. 6: The leading EOF of Northern Hemisphere 300-hPa winter (DJF) meridional wind (m s<sup>-1</sup> per std dev).

## North Atlantic Oscillation Response to Anomalous Indian Ocean SST in a Coupled GCM

JÜRGEN BADER

*Institute of Geophysics and Meteorology, University of Cologne, Cologne, and Max Planck Institute for Meteorology, Hamburg, Germany*

MOJIB LATIF

*Leibniz-Institute for Marine Sciences, University of Kiel, Kiel, Germany*

(Manuscript received 23 November 2004, in final form 4 April 2005)

### ABSTRACT

The dominant pattern of atmospheric variability in the North Atlantic sector is the North Atlantic Oscillation (NAO). Since the 1970s the NAO has been well characterized by a trend toward its positive phase. Recent atmospheric general circulation model studies have linked this trend to a progressive warming of the Indian Ocean. Unfortunately, a clear mechanism responsible for the change of the NAO could not be given. This study provides further details of the NAO response to Indian Ocean sea surface temperature (SST) anomalies. This is done by conducting experiments with a coupled ocean–atmosphere general circulation model (OAGCM). The authors develop a hypothesis of how the Indian Ocean impacts the NAO.

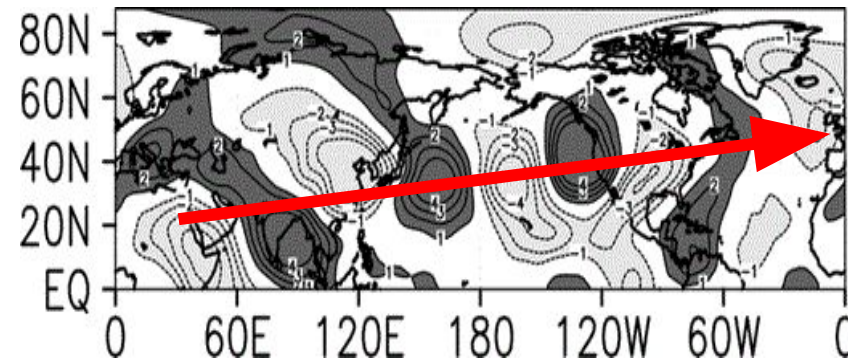
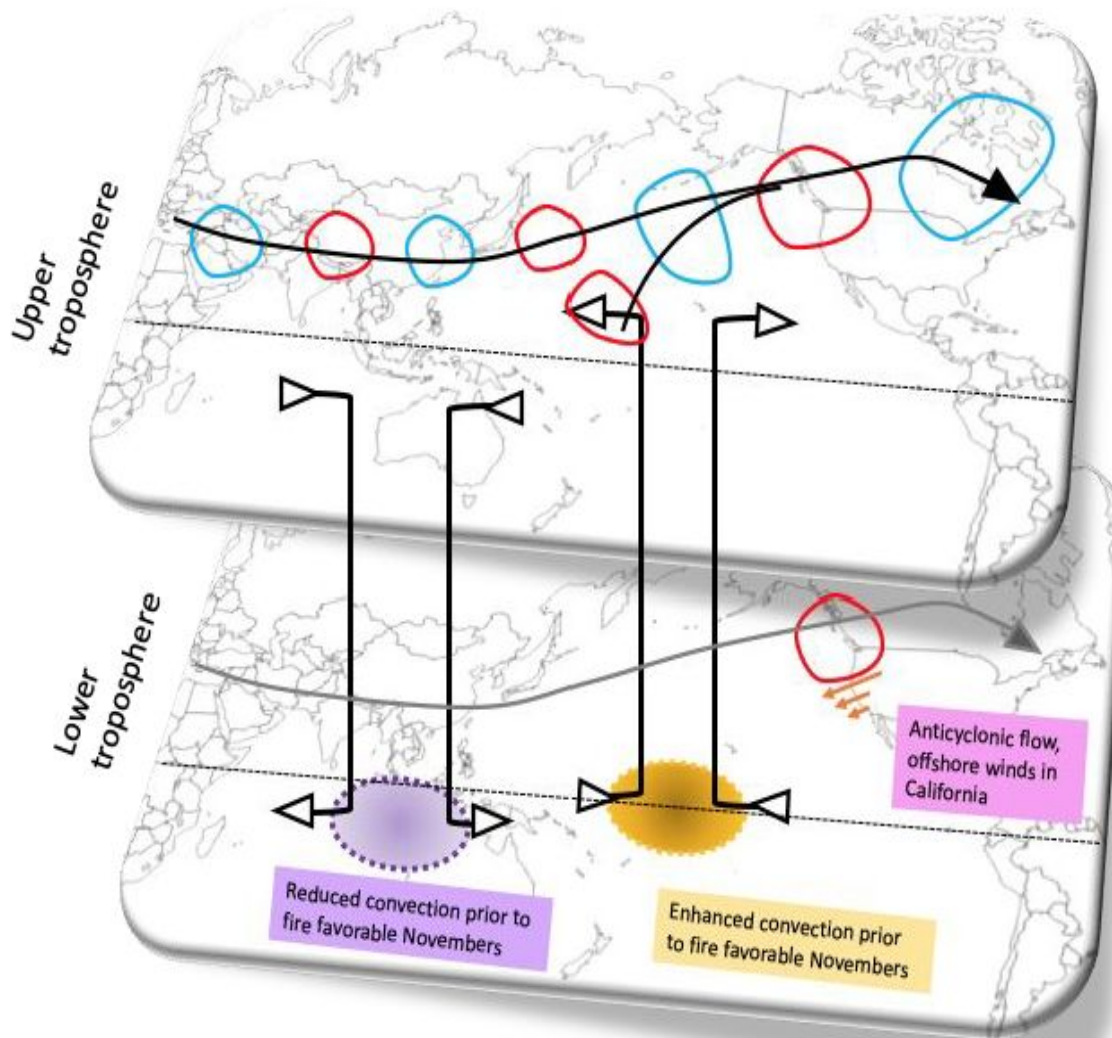


Fig. 14: Meridional 300-hPa winter (DJF) wind response for the “western Indian Ocean minus 1 K” experiment; units: m s<sup>-1</sup>.

Bader, J., and M. Latif, 2005: North Atlantic Oscillation Response to Anomalous Indian Ocean SST in a Coupled GCM. *J. Climate*, 18, 5382–5389, <https://doi.org/10.1175/JCLI3577.1>.

# IO can affect wildfire in California through a teleconnection pattern



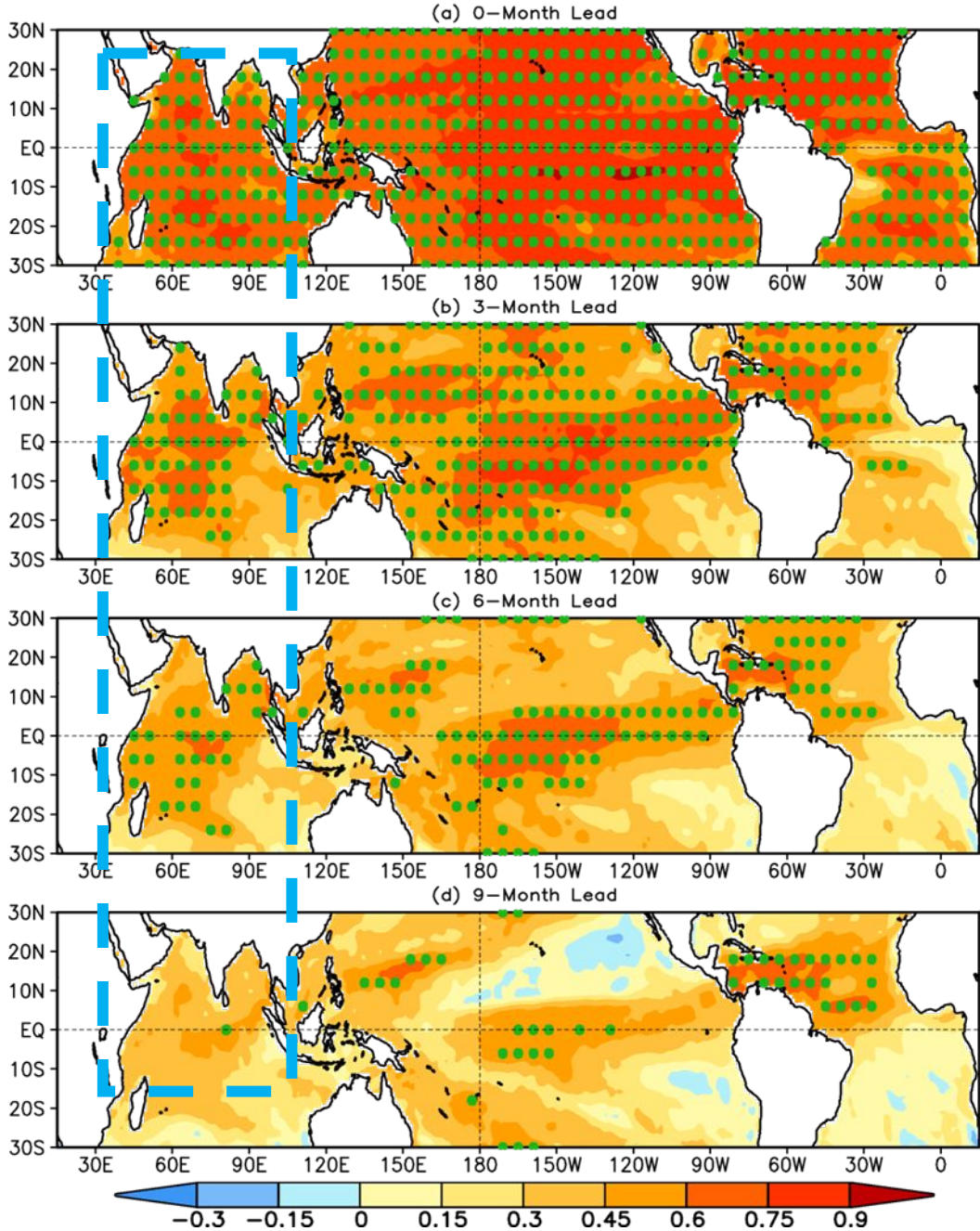
## Schematic: Interpretation of Dynamical Processes

**What could be causing ups/downs:** positive phase of Indian Ocean Dipole, El Niño Modoki

**What is most likely not causing ups/downs:** negative phase of Indian Ocean Dipole, La Niña Modoki, El Niño/La Niña

Dorsay, C., T. Murphree, K. Jones: Predicting Wildfire Favorable Conditions in California at Subseasonal to Seasonal Lead Times Using Remote Predictors. 2020 CDPW

SSTA Skill (CFSv2 20 Members; Jan1982~Dec2020; >0.5)



□ SSTA prediction skill is comparable in the tropical Indian and Pacific Oceans.

□ We can use model predicted DJF IOBM as a predictor to forecast SE CONUS winter precipitation.